

Optimizing Schedules for Quantum Annealing

Daniel Herr,^{1,2} Ethan Brown,¹ Bettina Heim,¹ Mario Könz,¹ Guglielmo Mazzola,¹ and Matthias Troyer^{1,3}

¹*Theoretische Physik, ETH Zurich, 8093 Zurich, Switzerland*

²*Quantum Condensed Matter Research Group, CEMS, RIKEN, Wako-shi 351-0198, Japan*

³*Quantum Architectures and Computation Group, StationQ, Microsoft Research, Redmond, WA 98052, USA*

Classical and quantum annealing are two heuristic optimization methods that search for an optimal solution by slowly decreasing thermal or quantum fluctuations. Optimizing annealing schedules is important both for performance and fair comparisons between classical annealing, quantum annealing, and other algorithms. Here we present a heuristic approach for the optimization of annealing schedules for quantum annealing and apply it to 3D Ising spin glass problems. We find that if both classical and quantum annealing schedules are similarly optimized, classical annealing outperforms quantum annealing for these problems when considering the residual energy obtained in slow annealing. However, when performing many repetitions of fast annealing, simulated quantum annealing is seen to outperform classical annealing for our benchmark problems.

Optimization is a fundamental task underlying many important problems in a wide range of disciplines. Solving an optimization problem means finding a configuration that (approximately) minimizes some cost function. This cost function can be interpreted as the Hamiltonian of a physical system and its minimization then corresponds to finding the ground state. In particular, discrete combinatorial optimization problems can be mapped [1, 2] to Ising spin glass problems, given by the Hamiltonian

$$H_P = - \sum_{i < j} J_{ij} s_i s_j - \sum_i h_i s_i. \quad (1)$$

Here, the spins $s_i = \pm 1$ are coupled pairwise through the J_{ij} terms and individually to external magnetic fields h_i . Finding the ground state of such Ising spin glass problems is a nondeterministic-polynomially (NP) hard problem [3] for which no efficient, polynomial time algorithms exist. Given the importance of these problems in many application areas, finding efficient optimization algorithms is an important endeavor.

One powerful heuristic algorithm to find low energy configurations of such a problem is simulated classical annealing (CA) [4, 5]. There, the system is first initialized to a random configuration at a high temperature and then gradually cooled during Monte Carlo simulations. This allows the system's configurations to escape from local minima and to thermally relax towards lower energy configurations [6].

Quantum annealing (QA) [7–11] is a related method, which has gained attention due to its implementation in commercial devices [12–14]. Instead of thermal fluctuations quantum fluctuations are used to drive the system out of local minima. During QA the system evolves from a trivial ground state of a quantum mechanical driver Hamiltonian \mathcal{H}_D to the solution of the problem Hamiltonian from Eq. (1). The evolution of the Hamiltonian is controlled by a parameter $s(t) \in [0, 1]$:

$$\mathcal{H} = s\mathcal{H}_P + (1 - s)\mathcal{H}_D. \quad (2)$$

This enables a transition from \mathcal{H}_D to \mathcal{H}_P . For this the Ising variables are represented by quantum spin-1/2 variables,

which results in

$$\mathcal{H}_P = - \sum_{i < j} J_{ij} \sigma_z^i \sigma_z^j - \sum_i h_i \sigma_z^i, \quad (3)$$

where σ_z^j is the Pauli- z matrices acting on spin j . The driver Hamiltonian is given by

$$\mathcal{H}_D = -\Gamma_0 \sum_i \sigma_x^i. \quad (4)$$

Alternatively one could just vary the transverse field Γ while \mathcal{H}_P is kept fixed:

$$\mathcal{H} = \mathcal{H}_P + (1 - s)\mathcal{H}_D. \quad (5)$$

We will use this schedule for our simulations.

We implement QA using a discrete time quantum Monte Carlo (QMC) simulation, because an exact simulation of QA is exponentially hard. We use the path integral Monte Carlo (PIMC) method to map a 3 dimensional quantum system into $3 + 1$ classical dimensions by the introduction of the imaginary time dimension [15]. It should be noted that this version of simulated quantum annealing (SQA), is indicative of the performance of a physical quantum annealer [16–19].

Recent comparisons between quantum and classical annealing for two-dimensional (2D) Ising spin glass systems have not shown any quantum speedup [20, 21]. The lack of speedup in this case may be due to the energy landscape of 2D spin glasses, with shallow but broad barriers that are easier to thermally surmount than to tunnel through [22].

Extending such simulations to three dimensions (3D) we find that whether classical or quantum annealing is better depends on the specific choice of annealing schedules. An apparent advantage of one method may simply be due to a bad or suboptimal choice of annealing schedule for the other method. To achieve a fair comparison both classical and quantum annealing schedules thus need to be fairly optimized. In this Letter we thus introduce a heuristic optimization method for quantum annealing, generalizing heuristics used to optimize classical annealing. We show that this heuristic leads to improvements over naïve schedules and allows fair comparisons of classical versus quantum annealing.

Adaptive Schedule In classical annealing the control parameter is the temperature, whose change over time is given by an annealing schedule. If the change is constant we call it a linear schedule and the update rule for the temperature is given by

$$\beta(t) = \beta_0 + \tilde{\lambda}t, \quad (6)$$

or in a discretized form

$$\beta_k = \beta_0 + \lambda k = \beta_{k-1} + \lambda, \quad (7)$$

where β_k is the inverse temperature at the k -th update sweep. For such a linear schedule, only the initial and final values of β may need to be optimized, with intermediate values that are obtained by linear interpolation.

Instead of guessing a schedule, one can determine optimized adaptive schedules by using a heuristic algorithm to optimize the schedule [23–25] in such a way that interesting regions where large changes to configurations may occur (e.g. close to phase transitions) are passed through more slowly.

An indicator for the size of a temperature step can be the specific heat

$$C_V = k_B \beta^2 \frac{d^2}{d\beta^2} \log Z = -k_B \beta^2 \frac{d}{d\beta} \langle E \rangle, \quad (8)$$

where Z is the partition function. C_V can be calculated from the fluctuation-dissipation theorem as

$$\beta^2 C_V \equiv \sigma \equiv -\frac{d}{d\beta} \langle E \rangle = \langle E^2 \rangle - \langle E \rangle^2. \quad (9)$$

In order to achieve a constant decrease in energy at each step, one aims for this quantity to be constant throughout the annealing process:

$$\frac{d\langle E \rangle}{dt} = -\lambda, \quad (10)$$

where the scale factor λ sets the targeted change in energy. The quantity $\langle E \rangle$ is only implicitly dependent on time through its dependence on the temperature, such that one can perform the chain rule

$$\frac{d\langle E \rangle}{d\beta} \frac{d\beta}{dt} = -\lambda. \quad (11)$$

Inserting Eq. (9) one obtains

$$\frac{d\beta}{dt} \sigma(\beta) = \lambda, \quad (12)$$

which can be discretized to obtain the an update rule for the adaptive schedule

$$\beta_{k+1} = \beta_k + \frac{\lambda}{\sigma_k}. \quad (13)$$

It can be observed that this schedule traverses slower in regions close to the phase transition, where C_V is large.

In order to derive a similarly optimized schedule for quantum annealing we use a quantity akin to the specific heat in classical systems. Starting from the quantum mechanical partition function

$$Z(s) = \text{tr} \left(e^{-\beta \mathcal{H}(s)} \right) \quad (14)$$

we first derive an adaptive schedule for Eq. (2). Substituting the derivative with respect to β by one with respect to the quantum control parameter s in Eq. (8) we define

$$C(s) = \frac{1}{\beta} \frac{d^2}{ds^2} \log(Z), \quad (15)$$

which will determine the annealing schedule. Performing the derivatives we obtain

$$\begin{aligned} C(s) &= -\frac{d}{ds} \langle \mathcal{H}_P - \mathcal{H}_D \rangle_s \\ &= \beta \left(\langle (\mathcal{H}_P - \mathcal{H}_D)^2 \rangle_s - \langle \mathcal{H}_P - \mathcal{H}_D \rangle_s^2 \right) \end{aligned} \quad (16)$$

Note, that the expectation values in this equation are dependent on the parameter s . Similar to the classical procedure, we aim for a constant change in time:

$$\frac{ds}{dt} C(s) = \lambda. \quad (17)$$

Thus we obtain an update rule for the quantum annealing schedule:

$$s_{k+1} = s_k + \frac{1}{\beta} \frac{\lambda}{\sqrt{\langle (\mathcal{H}_P - \mathcal{H}_D)^2 \rangle_s - \langle \mathcal{H}_P - \mathcal{H}_D \rangle_s^2}} \quad (18)$$

For the alternative quantum annealing procedure of Eq. (5), a similar derivation leads to a simpler rule

$$s_{k+1} = s_k + \frac{1}{\beta \Gamma_0} \frac{\lambda}{\sqrt{1 - \langle \sigma_x \rangle_s^2}}. \quad (19)$$

Note that Γ_0 corresponds to the initial transverse field of the annealing schedule and an appropriate value needs to be determined before any efficient annealing run.

For classes of random instances one does not optimize the schedule for each individual instance but instead optimizes over the average of a limited set of instances, and use the average of this set to define an adaptive schedule for the entire class.

Results In the remainder of this work we will use the latter schedule, obtained by an ensemble average of $\langle \sigma_x \rangle_s$ over a set of 1000 random, uniformly distributed 3D Ising spin glass instances on a simple cubic lattice. We investigate 3D spin glasses because of the argument [22] that random 3D Ising spin glasses are more likely to profit from quantum tunneling since they exhibit a non-zero temperature phase transition [26].

In Figure 1 we we show the expectation value of the denominator of the step size, averaged over 1000 instances. In

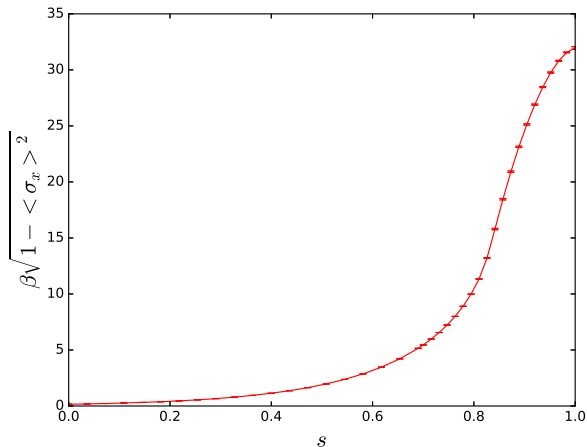


Figure 1. Expectation value of the step size denominator as a function of s . Thus it can be seen, that initially, for small values of s annealing proceeds fast and slows down towards the end. Measurements were performed at $\beta = 32$ and $\Gamma_0 = 10$. The expectation value for this plot was obtained using a set of 100 random 3D Ising instances with couplings chosen uniformly from $[-1, 1]$. The transverse field relates to the control parameter with $\Gamma(s) = (1 - s) \Gamma_0$.

the beginning, when the transverse field is strong, the system is close to an eigenstate of σ_x and the problem Hamiltonian does not influence the dynamics much. Thus, the step size is large.

In order to find an optimized schedule, the transverse field Γ_0 has to be optimized. This corresponds to an optimization of the starting value of the schedule and yielded $\Gamma_0 = 1.5$. The final value of the transverse field needs to be $\Gamma = 0$ in order to recover the problem Hamiltonian at the end of the annealing process.

Figure 2 shows the linear and the adaptive schedules for optimized and unoptimized initial field Γ_0 . Consistent with Fig. 1 one can see that the adaptive schedules are slower in regions, where the transverse field is weak. The residual energy of these schedules is shown Fig 3, which demonstrates improved performance of the adaptive schedules over the linear ones. The improvement is especially large if one starts with unoptimized large initial transverse fields Γ_0 . In those cases the adaptive schedule quickly reduces the transverse field and then slows down when entering the interesting parameter region. Conversely, one can see in Figure 4 that, for an optimized Γ_0 the optimized schedule is close to a linear one, with similar performance.

Since neither CA nor QA are guaranteed to find the exact ground state, we will first investigate the residual energy $E_{\text{res}} = E - E_0$ as a metric to compare the efficiency of different annealing schemes. It is defined as the difference between the energy of the (local) minimum E found in an annealing run and the ground state energy E_0 . The residual energy is a function of annealing time t_a , which in our simulations is given in units of Monte Carlo sweeps. The behavior of SQA

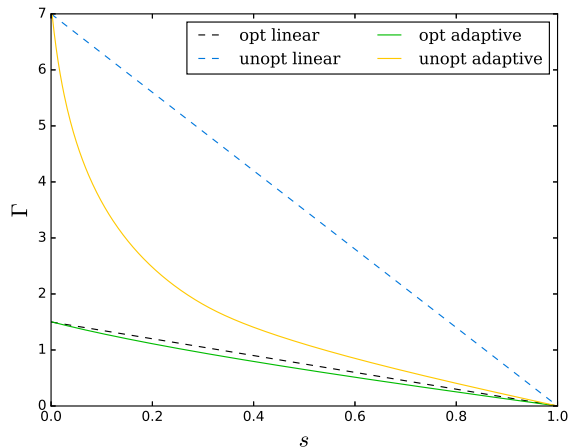


Figure 2. Plot of linear schedule and adaptive schedules with optimized and unoptimized initial transverse Field Γ_0 . Close to the optimal values ($\Gamma_0 \approx 1.5$) one can see only minor differences in the two schedules, but for unoptimized starting values ($\Gamma_0 = 7$) the adaptive schedule anneals much faster at the beginning such that less time is spent in unimportant regions.

on 3D Ising spin glasses is similar to that of 2D Ising spin glasses [21]. SQA, running fast, can initially lower the energy much faster than CA but tends to get stuck in local minima. Figure 4 shows that this initial fast convergence happens earlier with higher temperature. Yet, for every choice of inverse temperature, SQA suffers from getting stuck in local minima. CA does not display this problem, which is why CA outperforms any SQA run after sufficient annealing time.

As an alternative approach to slow annealing, many fast annealing runs might be beneficial for some problems [27]. The

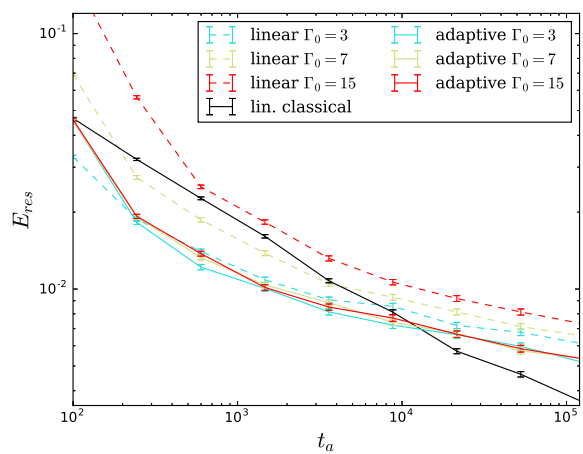


Figure 3. Comparison of median residual energy between linear and adaptive schedules at different starting values Γ_0 . The linear schedule steadily degrades with increasingly suboptimal Γ_0 whereas the adaptive schedule degrades only slightly.

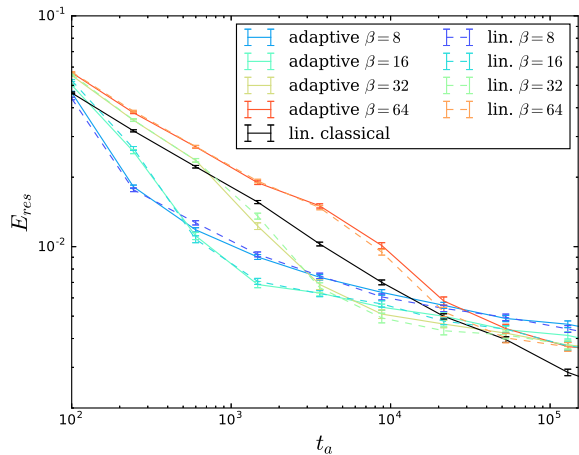


Figure 4. Comparison of median residual energy for different values of β between adaptive, linear QA schedules and linear CA. One can see almost no qualitative difference between the two schedules when only optimized parameters are used.

total effort here is the product of the annealing time and the number of repetitions R required to find the ground state with a probability \bar{s} . Denoting the probability to find the ground state in a single execution by p the required number of repetitions is $R = \log(1 - p)/\log(1 - \bar{s})$ [20]. To compare the different annealing approaches we choose t_a to optimize the total computational effort $t_a \cdot R$ for each system size.

Results for repeated fast annealing are shown in Fig. 5. We observe a slight scaling advantage for SQA over CA.

Apart from the proposed adaptive schedule, we performed a comparison of different nonlinear parameterizations of annealing schedules for QA, but found for optimized parameters no speedup compared to the linear schedule for any of them. The analysis for these and further simulations can be found in the supplementary material.

Conclusion For fair comparisons both CA and QA need to be optimized, otherwise wrong conclusions for the efficiency are drawn. To achieve this goal we proposed a heuristic nonlinear schedule and demonstrated that it is resistant against sub-optimally chosen initial values for the transverse field Γ_0 on random 3D Ising spin glasses.

A comparison between CA and QA for 3D Ising spin glasses gives similar results as in 2D. The existence of a finite temperature phase transition does not have a major influence on the relative performance between CA and QA. While QA rapidly finds a low energy local minimum, increasing the annealing time leads to CA finding lower energy states. A similar conclusion is drawn in Ref. [28], where quantum speed-up is obtained in the random ferromagnetic Ising chain model, i.e. a system for which CA encounters no phase-transition at any finite temperature, while QA does.

Using many short runs, our simulations showed an advantage for the scaling of SQA over CA. Our simulations were restricted to relatively small system sizes, because the exact

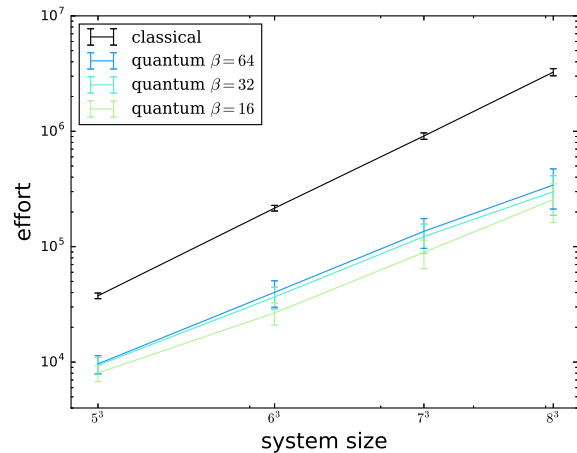


Figure 5. Scaling properties for QA and CA: Median effort to find the ground state with probability 90%. Since these are simulations, the performance of the real machine may differ by some constant factor. Still, a scaling advantage can be observed. For a confidence level of 95% our regression gave a classical slope of 0.650 ± 0.003 and for the quantum case the slope is given by 0.51 ± 0.06 for $\beta = 16$. The slope of $\beta = 32$ is given by 0.52 ± 0.06 , and the slope of $\beta = 64$ is given by 0.54 ± 0.07 both are calculated with the same confidence as for CA.

ground state had to be calculated beforehand. Surface effects of these small instances might skew the observed scaling behavior such that a verification of our results for larger instances should be performed.

Extending our analysis to different problem classes will give further insight to where (S)QA gains an advantage over CA.

Acknowledgments We thank the spinglass server [29] for their calculation of the ground state energy. We also thank Ilia Zintchenko for interesting discussions and the whiplash framework for easier management of measurement data. MT acknowledges hospitality of the Aspen Center for Physics, supported by NSF grant PHY-1066293. This paper is based upon work supported in part by the Swiss National Science Foundation through NCCR QSIT and by ODNI, IARPA via MIT Lincoln Laboratory Air Force Contract No. FA8721-05-C-0002.

-
- [1] A. Lucas, *Frontiers in Physics* **2** (2014), 10.3389/fphy.2014.00005.
 - [2] M. Troyer, B. Heim, E. Brown, and D. Wecker, in *APS Meeting Abstracts* (2015).
 - [3] F. Barahona, *Journal of Physics A: Mathematical and General* **15**, 3241 (1982).
 - [4] S. Kirkpatrick, C. D. Gelatt, and M. P. Vecchi, *Science* **220**, 671 (1983).
 - [5] N. Metropolis, A. W. Rosenbluth, M. N. Rosenbluth, A. H. Teller, and E. Teller, *The Journal of Chemical Physics* **21**, 1087

- (1953).
- [6] D. Bertsimas and J. Tsitsiklis, *Statistical Science* **8**, 10 (1993).
- [7] P. Ray, B. K. Chakrabarti, and A. Chakrabarti, *Physical Review B* **39**, 11828 (1989).
- [8] A. B. Finnila, M. A. Gomez, C. Sebenik, C. Stenson, and J. D. Doll, *Chemical Physics Letters* **219**, 343 (1994).
- [9] T. Kadowaki and H. Nishimori, *Physical Review E* **58**, 5355 (1998).
- [10] E. Farhi, J. Goldstone, S. Gutmann, J. Lapan, A. Lundgren, and D. Preda, *Science* **292**, 472 (2001).
- [11] A. Das and B. K. Chakrabarti, *Rev. Mod. Phys.* **80**, 1061 (2008).
- [12] P. I. Bunyk, E. M. Hoskinson, M. W. Johnson, E. Tolkacheva, F. Altomare, A. J. Berkley, R. Harris, J. P. Hilton, T. Lanting, A. J. Przybysz, and J. Whittaker, *IEEE Transactions on Applied Superconductivity* **24**, 1 (2014).
- [13] R. Harris, M. W. Johnson, T. Lanting, A. J. Berkley, J. Johansson, P. Bunyk, E. Tolkacheva, E. Ladizinsky, N. Ladizinsky, T. Oh, F. Cioata, I. Perminov, P. Spear, C. Enderud, C. Rich, S. Uchaikin, M. C. Thom, E. M. Chapple, J. Wang, B. Wilson, M. H. S. Amin, N. Dickson, K. Karimi, B. Macready, C. J. S. Truncik, and G. Rose, *Phys. Rev. B* **82**, 024511 (2010).
- [14] M. W. Johnson, M. H. S. Amin, S. Gildert, T. Lanting, F. Hamze, N. Dickson, R. Harris, a. J. Berkley, J. Johansson, P. Bunyk, E. M. Chapple, C. Enderud, J. P. Hilton, K. Karimi, E. Ladizinsky, N. Ladizinsky, T. Oh, I. Perminov, C. Rich, M. C. Thom, E. Tolkacheva, C. J. S. Truncik, S. Uchaikin, J. Wang, B. Wilson, and G. Rose, *Nature* **473**, 194 (2011).
- [15] M. Suzuki, *Progress of Theoretical Physics* **56**, 1454 (1976).
- [16] G. Mazzola, V. N. Smelyanskiy, and M. Troyer, arXiv (2017), arXiv:1609.04673.
- [17] S. V. Isakov, G. Mazzola, V. N. Smelyanskiy, Z. Jiang, S. Boixo, H. Neven, and M. Troyer, *Phys. Rev. Lett.* **117**, 180402 (2016).
- [18] Z. Jiang, V. N. Smelyanskiy, S. V. Isakov, S. Boixo, G. Mazzola, M. Troyer, and H. Neven, *Phys. Rev. A* **95**, 012322 (2017).
- [19] V. S. Denchev, S. Boixo, S. V. Isakov, N. Ding, R. Babbush, V. Smelyanskiy, J. Martinis, and H. Neven, *Phys. Rev. X* **6**, 031015 (2016).
- [20] T. F. Rønnow, Z. Wang, J. Job, S. Boixo, S. V. Isakov, D. Wecker, J. M. Martinis, D. A. Lidar, and M. Troyer, *Science* **345**, 420 (2014), <http://www.sciencemag.org/content/345/6195/420.full.pdf>.
- [21] B. Heim, T. F. Rønnow, S. V. Isakov, and M. Troyer, *Science* **348**, 215 (2015), <http://www.sciencemag.org/content/348/6231/215.full.pdf>.
- [22] H. G. Katzgraber, F. Hamze, and R. S. Andrist, *Phys. Rev. X* **4**, 021008 (2014).
- [23] F. R. Huang, M.D. and A. Sangiovanni-Vincentelli, in *Proc. IEEE Int. Conference on Computer-Aided Design* (Santa Clara, 1986) pp. 381–384.
- [24] P. J. van Laarhoven and E. H. Aarts, *Simulated Annealing: Theory and Applications* (Springer Netherlands, 1987).
- [25] T. H. Fischer, W. P. Petersen, and H. P. L thi, **16**, 923 (1995).
- [26] J. Bricmont and A. Kupiainen, *Communications in Mathematical Physics* **116**, 539 (1988).
- [27] D. S. Steiger, T. F. Rønnow, and M. Troyer, *Phys. Rev. Lett.* **115**, 230501 (2015).
- [28] T. Zanca and G. E. Santoro, *Phys. Rev. B* **93**, 224431 (2016).
- [29] COPhy and M. Jünger, “Spin Glass Server,” <http://www.informatik.uni-koeln.de/spinglass/> (accessed 2016).